

RESEARCH ARTICLE



WILEY

Three-dimensional geometric morphometric analysis of the distal radius insertion sites of the palmar radiocarpal ligaments in hominoid primates

Aroa Casado¹ | Vicenç Punsola¹ | Mónica Gómez¹ | Marina de Diego¹ | Mercedes Barbosa² | Félix J. de Paz² | Juan F. Pastor² | Josep M. Potau¹

¹Unit of Human Anatomy and Embryology, University of Barcelona, Barcelona, Spain

²Department of Anatomy and Radiology, University of Valladolid, Valladolid, Spain

Correspondence

Josep M. Potau, Unit of Human Anatomy and Embryology, University of Barcelona, C/Casanova 143, 08036 Barcelona, Spain. Email: jpotau@ub.edu

Funding information

European Regional Development Fund, Grant/Award Number: CGL2014-52611-C2-2-P; Ministerio de Economía y Competitividad; Universitat de Barcelona, Grant/Award Number: APIF-UB 2016/2017

Abstract

Objectives: To identify anatomic differences in the insertion sites of the palmar radiocarpal ligaments in different species of hominoid primates that may be related to their different types of locomotion.

Materials and methods: We have used three-dimensional geometric morphometrics (3D GM) to analyze the distal radius ligament insertion sites in 31 *Homo sapiens*, 25 *Pan troglodytes*, 31 *Gorilla gorilla*, and 15 *Pongo pygmaeus*. We have also dissected the radioscaphocapitate (RSC), long radiolunate (LRL) and short radiolunate (SRL) ligaments in six *H. sapiens* and five *P. troglodytes* to obtain quantitative values that were then compared with the results of the 3D GM analysis.

Results: *H. sapiens* had a relatively larger insertion site of the RSC + LRL ligament than the other hominoid primates. *P. pygmaeus* and *P. troglodytes* had a relatively large SRL ligament insertion site with a palmar orientation. In *G. gorilla*, the two ligament insertion sites were relatively smaller and the SRL insertion site had an ulnopalmar orientation.

Discussion: The morphological differences observed can be related to the types of locomotion used by the different species and to quantitative data obtained from the dissection of ligaments in *H. sapiens* and *P. troglodytes*. 3D GM analysis of ligament insertion sites can help in interpreting the types of locomotion used by extinct hominoid primates through the analysis of preserved fossilized fragments of the distal radius.

KEYWORDS

distal radius, hominoid primates, radiocarpal ligaments

1 | INTRODUCTION

The radiocarpal joint is an important functional element of the wrist, especially in primates, since it combines the flexibility needed for manipulatory functions and the shock-absorbing capacity to compensate for stresses generated during locomotion (Whitehead, 1993). The distal radial epiphysis, a key element in the radiocarpal joint, has different characteristics among primates of the Hominoidea superfamily,

such as gibbons, orangutans, gorillas, chimpanzees, bonobos and humans (Gebo, 2014), which may be related to the different types of locomotion developed by these primates. For example, anatomic adaptations of the distal radial epiphysis in knuckle-walkers, such as chimpanzees and gorillas, include the distal projection of its dorsal edge, which limits the extension of the wrist (Jenkins & Fleagle, 1975; Richmond & Strait, 2000) while increasing its stability and its weight-bearing capacity (Richmond, Begun, & Strait, 2001). These adaptations

are not found in gibbons or orangutans, which use mainly suspensory locomotion, or in human bipeds, who use their upper extremities fundamentally for the manipulation of objects (Gebo, 2014). However, other studies have found that the morphology of the distal radial epiphysis does not reliably explain the types of locomotion developed by the different species of hominoid primates (Tallman, 2012) since the projection of the dorsal ridge is similar in African and Asian apes (Orr, 2017) and is different only in *Homo sapiens*, where it is less marked.

Unlike other bones of the upper extremity, such as the proximal humeral epiphysis (Arias-Martorell, Potau, Bello-Hellegouarch, Pastor, & Pérez-Pérez, 2012), the distal radial epiphysis does not have well-defined muscle insertion sites that could be used to relate morphological differences to different types of locomotion. However, in the distopalmar region of the distal radial epiphysis, there are two insertion sites of three ligaments that stabilize the radiocarpal joint (Figure 1). Together, these three ligaments form the palmar radiocarpal ligament, as it is called in classic anatomical nomenclature (Figure 2). On the palmar side of the styloid process and the palmar edge of the scaphoid fossa, there is an insertion site common to the radioscapocapitate (RSC) and long radiolunate (LRL) ligaments, while at the palmar edge of the lunate fossa, there is an insertion site for the short radiolunate ligament (SRL) (Apergis, 2013). The RSC ligament is inserted proximally on the palmar side of the styloid process of the radius and distally on the scaphoid and the capitate bone (Buijze, Dvinskikh, Strackee, Streekstra, & Blankevoort, 2011; Buijze, Lozano-Calderon, Strackee, Blankevoort, & Jupiter, 2011); the LRL ligament runs between the palmar edge of the scaphoid fossa of the radius and the lunate (Berger, 2010); the SRL ligament spans the palmar edge of the lunate fossa of the radius and the lunate. These three ligaments are considered the main stabilizing elements of the radiocarpal joint (Apergis, 2013) and in humans they are more developed than the dorsal ligaments (Apergis, 2013; Mayfield et al., 1979; Nordin & Frankel, 2001). Jointly, the three ligaments limit dorsal rotation and translation of the carpus (Katz, Green, Werner, & Loftus,

2003) and tighten during wrist extension. In addition, the RSC and LRL ligaments are an important stabilizing element of the radial region of the wrist (Cardoso & Szabo, 2007). The RSC ligament stabilizes the scaphoid, while the LRL and SRL ligaments stabilize the lunate (Apergis, 2013; Bateni, Bartolotta, Richardson, Mulcahy, & Allan, 2013; Cardoso & Szabo, 2007; Nordin & Frankel, 2001; Ringler & Murthy, 2015; Short, Werner, Green, & Masaoka, 2002; Short, Werner, Green, Sutton, & Brutus, 2007). The stabilizing function of the ligaments RSC, LRL, and SRL is of great importance during extension and ulnar deviation of the wrist because they limit the movements of extension and ulnar deviation affecting the scaphoid and the lunate in these cases (Apergis, 2013; Short et al., 2002; Short et al., 2007).

The anatomic and functional characteristics of the wrist ligaments of hominoid primates have not been extensively explored, since muscles and bones have been given higher priority. The few analyses of the morphology of the wrist ligaments in hominoid primates, performed in the context of studies of anatomic adaptations that stabilize the wrist in primate knuckle-walkers, have found that the palmar region of the wrist joint capsule is extremely thick due to the development of the ligaments attaching the radius to the carpal bones (Tuttle, 1967; Tuttle, 1969). This development can explain the limited extension of the wrist movement in primate knuckle-walkers (Jenkins & Fleagle, 1975; Orr, 2017; Richmond & Strait, 2000) and ensures the stability of the wrist during the support phase of knuckle-walking (Richmond & Strait, 2000).

Unlike African great apes, orangutans have a more mobile wrist joint with a greater degree of extension, which allows them to move through the trees using quadrupedal palmigrade locomotion (Orr, 2017; Thorpe & Crompton, 2007). An anatomical feature of the wrist of orangutans, which they share with chimpanzees, is the relatively large articular surface of the lunate (Kivell, Barros, & Smaers, 2013), an adaptation that enables them to bear the loads that are put on the radiolunate joint of the wrist during its ulnar deviation, a characteristic posture in vertical climbing (Heinrich, Rose, Leakey, & Walker, 1993; Sarmiento, 1988).



FIGURE 1 The distal radial epiphysis in *Homo sapiens*. 1 = insertion site of the radioscapocapitate and long radiolunate ligaments. 2 = insertion site of the short radiolunate ligament

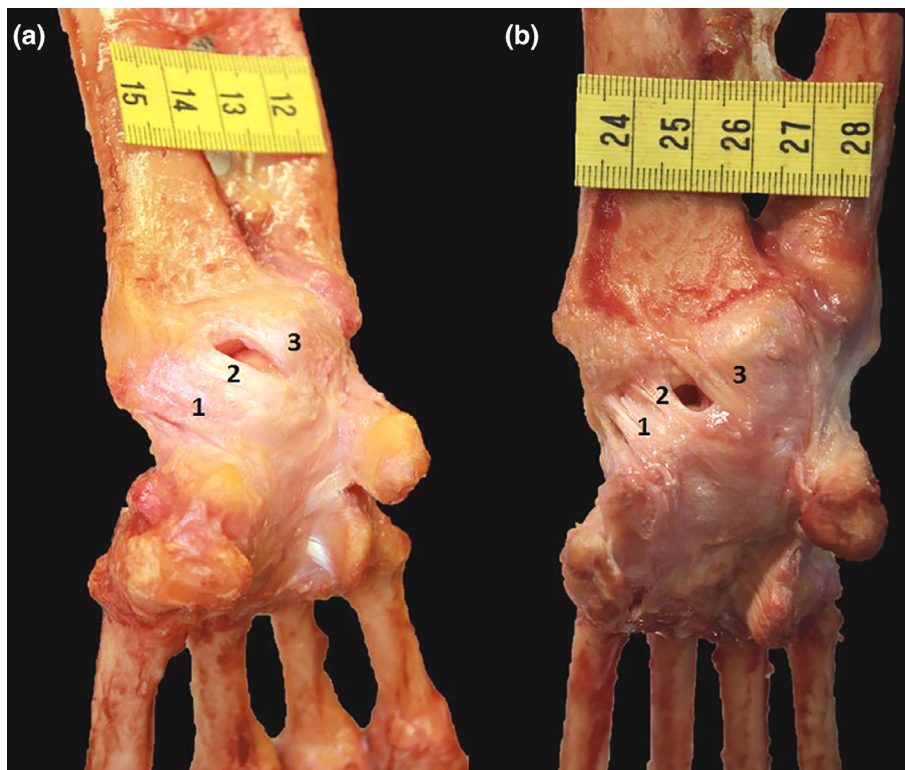


FIGURE 2 Dissection of the palmar radiocarpal ligament in (a) *Homo sapiens* and (b) *Pan troglodytes*.

1 = radioscaphocapitate ligament, 2 = long radiolunate ligament, 3 = short radiolunate ligament

We have carried out a three-dimensional geometric morphometrics (3D GM) analysis of the two insertion sites of the major ligaments stabilizing the radiocarpal joint in different species of hominoid primates. We hypothesized that the morphology of these insertion sites would be modified as a result of anatomic differences in the ligaments, which would in turn arise from functional differences due to different forms of locomotion. Our main objective was to identify differential morphological patterns in the insertion sites of the RSC + LRL and SRL ligaments in humans (*H. sapiens*), orangutans (*Pongo pygmaeus*), chimpanzees (*Pan troglodytes*), and gorillas (*Gorilla gorilla*) that could be related to their different types of locomotion. We believe that these results will help expand our present knowledge of the wrist anatomy and function of hominoid primates, especially at the level of bones and ligaments. We also believe that our results will be useful in different fields, such as comparative anatomy, evolutionary anatomy, and anthropology, since they can be useful in interpreting the types of locomotion used by extinct hominoid primates through the analysis of preserved fossilized fragments of the distal radial epiphysis.

2 | MATERIALS AND METHODS

2.1 | Osteological samples

We included a total of 102 left radii in the study: 31 *H. sapiens* (12 males and 19 females); 31 *G. gorilla* (17 males and 14 females); 25 *P. troglodytes* (11 males, 13 females, and one individual of undetermined sex); and 15 *P. pygmaeus* (8 males and 7 females) (Table 1). All nonhuman primate bones came from the University of

TABLE 1 Bone samples used for the 3D GM analysis

Sample	N	Male	Female	Collection
<i>Homo sapiens</i>	31	12	19	UB
<i>Gorilla gorilla</i>	31	17	14	AIM
<i>Pan troglodytes</i>	25 ^a	11	13	AIM
<i>Pongo pygmaeus</i>	15	8	7	AIM
TOTAL	102	48	53	

Abbreviations: 3D GM, 3D geometric morphometrics; AIM, University of Zurich Anthropological Institute and Museum; UB, University of Barcelona.

^aOne sample of *Pan troglodytes* was from an individual of undetermined sex.

Zurich Anthropological Institute and Museum, Switzerland and were from adult individuals reared in the wild. The human samples came from the Unit of Human Anatomy and Embryology of the University of Barcelona, Spain and were from adults aged between 38 and 97 years (average age of 80.9 years).

2.2 | 3D GM analysis

Each distal radial epiphysis, where the two insertion sites of the RSC + LRL and SRL ligaments are located, was scanned with a 3D Next Engine Ultra HD laser surface scanner, at a resolution of 0.1 mm space-point separation with a density of 40 k (2x) points. The different sections of the scans were fused with the Volume Merge option of the Next Engine HD software at a resolution of 0.5 mm and saved as a PLY file. The resulting triangle mesh was edited with the open-

source MeshLab software (Cignoni et al., 2008) and the models were imported into the Landmark Editor software (v. 3.6) (Wiley, 2006) for placing the landmarks.

We used a set of nine Type II and one Type III landmarks (Table 2) to represent the morphology of the two insertion sites of the RSC + LRL and SRL ligaments in the distal epiphysis of the radius. The L1–L4 landmarks defined the insertion site of the SRL ligament, while the L5–L10 landmarks define the insertion site of the RSC + LRL ligaments (Figure 3).

The raw data obtained with the Landmark Editor software based on the landmark coordinates were exported into the MorphoJ statistical package (Klingenberg, 2011). First, a generalized Procrustes analysis (GPA) was used to eliminate variability due to differences of size, placement, or orientation and to minimize the sum of square distances between equivalent landmarks (Bookstein, 1991; O'Higgins, 2000; Zelditch, Swiderski, Sheets, & Fink, 2004). This procedure allows the resulting data, termed Procrustes residuals, to be used in a multivariate analysis (Rohlf & Marcus, 1993; Zelditch et al., 2004). A principal components analysis (PCA) was then performed in order to reduce complex multidimensional data to fewer components, or eigenvectors, that could be used to explain the main differences between groups (Klingenberg, 2011; O'Higgins, 2000; Zelditch et al., 2004). Finally, a linear discriminant analysis (LDA) was used to determine the statistical significance of the differences in shape identified by the PCA, with Fisher's classification rule and a leave-one-out, jackknife cross-validation method to obtain the post hoc probabilities of correct classification (Klingenberg, 2011). Parametric T-square tests with permutation were performed to compare group means within the LDA in MorphoJ (Klingenberg, 2011).

In order to determine the influence of size on variation in shape (allometric scaling), a multivariate regression analysis (MRA) was performed, with the main principal component, indicative of shape, as the dependent variable and the centroid size (CS), indicative of size, as the independent variable (Bookstein, 1991; Klingenberg, 2011; O'Higgins, 2000; Zelditch et al., 2004). MorphoJ can carry out multivariate regressions with a permutation test with 1,000 randomizations and pool the regression within defined subgroups (the four species in the present study) as an external variable, which makes it an ideal procedure when a correction for size between groups is necessary.

In order to obtain more robust results, we also used the 3D scans of the distal radial epiphysis to obtain quantitative data on the ligament insertion sites. We used MeshLab to calculate the surface area of the insertion sites of the RSC + LRL and SRL ligaments in mm² (RSC + LRLiss and SRLiss), and we normalized these values relative to the surface area of the distal articular surface (DAS) of the radius (RSC + LRLiss/DAS and SRLiss/DAS). The values obtained from the surface areas of the DAS were also used to perform a second MRA using SPSS 22, with the first three principal components obtained from our 3D GM analysis, indicative of shape, as the dependent variable, and the distal articular surface, indicative of size, as the independent variable. Quantitative data for the orientation of the two ligament insertion sites was also obtained by calculating the angle formed by the main axis of each site and the transversal axis of the distal radial epiphysis (RSC + LRLa and SRLa). To

TABLE 2 Numbering, description and types of landmarks (O'Higgins, 2000)

Landmark	Type	Description
1	II	Most distal-ulnar point of the SRL ligament insertion area
2	II	Most proximal-ulnar point of the SRL ligament insertion area
3	II	Most distal-radial point of the SRL ligament insertion area
4	II	Most proximal-radial point of the SRL ligament insertion area
5	II	Most distal-ulnar point of the RSC + LRL ligaments insertion area
6	II	Most proximal-ulnar point of the RSC + LRL ligaments insertion area
7	II	Most proximal-radial point of the RSC + LRL ligaments insertion area
8	II	Most radial point of the RSC + LRL ligaments insertion area
9	II	Most distal-radial point of the RSC + LRL ligaments insertion area
10	III	Intermediate point between landmarks 5 and 9

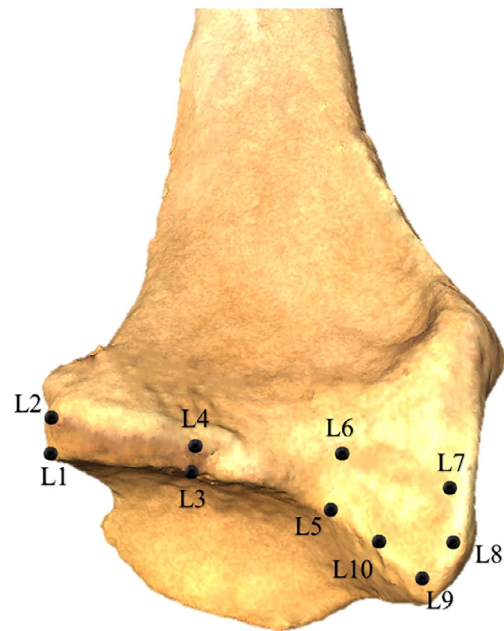


FIGURE 3 Three-dimensional model of the distal epiphysis of the radius in *Homo sapiens* showing the location of the landmarks used

undertake this, distal views of the 3D scans were used, in which the principal axes of the ligament insertion sites and the transversal axis of the distal radial epiphysis were plotted (Figure 4). The principal axis of the insertion site of the RSC + LRL ligaments was plotted by linking the intermediary points between landmarks L1–L2 and L3–L4; the principal axis of the insertion site of the SRL ligament was plotted by linking the landmarks L6 and L8; the transversal axis of the distal radial epiphysis

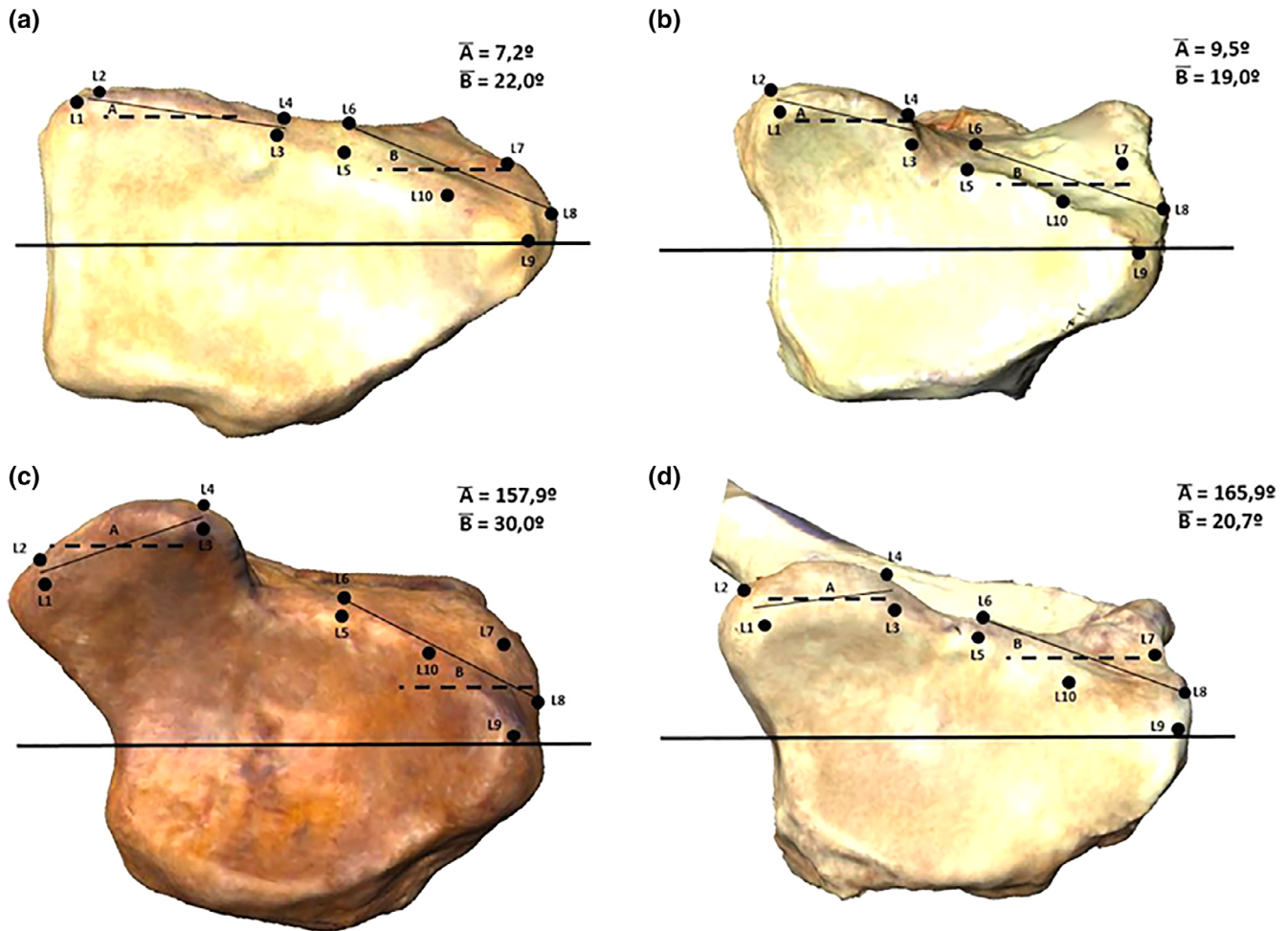


FIGURE 4 Calculation of the orientation angles for the SRL (A) and RSC + LRL (B) ligament insertion sites in *Homo sapiens* (a), *Pongo pygmaeus* (b), *Gorilla gorilla* (c), and *Pan troglodytes* (d). \bar{A} = average value of the orientation angle of the SRL ligament insertion site. \bar{B} = average value of the orientation angle of the RSC + LRL ligaments insertion site. The thick continuous line represents the transversal axis of the distal radial epiphysis; the thin continuous lines represent the principal axes of the SRL and RSC + LRL ligaments insertion sites; the dotted lines represent the palmar projections of the transversal axis of the distal radial epiphysis

was plotted by joining the styloid process and the midpoint of the ulnar notch. Following this, the transversal axis was palmarly projected until it bisected the principal axes of the ligament insertion sites and the delimited angle between each principal axis and the transversal axis was calculated using the ImageJ software (Rueden et al., 2017).

Finally, we performed a phylogenetic correction analysis to examine whether the degree of relationship between the four species of great apes influenced the morphological changes in the ligament insertion sites (Almécija & Alba, 2014). The molecular phylogeny of the species considered was derived from the 10kTrees website (Arnold, Matthews, & Nunn, 2010) and analyzed with MorphoJ (Perelman et al., 2011).

2.3 | Palmar ligament samples

The palmar ligaments of the radiocarpal joint (RSC, LRL, and SRL) were dissected in six *H. sapiens* and in five *P. troglodytes* (Figure 2). The six human samples came from the Body Donation Service of the University of Barcelona and corresponded to four males and two females

with an average age of 86.5 years (range, 81–94 years). None of the selected individuals showed signs of degeneration, inflammation, or fracture of the bones or joints, or signs of atrophy or muscle injury. The five chimpanzees came from the Anatomy Museum of the University of Valladolid, Spain and corresponded to an adult male and four adult females from different Spanish zoos, all of which had died from causes unrelated to the present study. All samples, both humans and chimpanzees, had been cryopreserved without fixation within 24–48 hr post mortem.

The same researcher (JMP) dissected the upper extremities of each individual, obtaining quantitative information of the ligaments and muscles of the main complex joints of the upper extremity. He dissected and identified the ligaments of the radiocarpal joint and weighed them on a precision scale. Once he had obtained the absolute weights of the RSC + LRL (RSC + LRLw) ligaments and the SRL ligament (SRLw) in grams, these weights were normalized with respect to a representative value of the size of the distal radius (R), obtained by multiplying its transverse and sagittal diameters (RSC + LRLw/R and SRLw/R). He then calculated the

total weight of each individual's radiocarpal joint ligaments and this value was used to obtain the percentage of the total weight represented by the RSC + LRL ligaments (%RSC + LRL) and SRL ligament (%SRL). Finally, he photographed the RSC + LRL and SRL ligaments with a Canon EOS-50 digital camera in order to calculate their surface area (RSC + LRLs and SRLs) with ImageJ.

In addition to this quantitative information on the wrist ligaments, we also obtained information about the relative weight of the flexor carpi radialis (FCR) and abductor pollicis longus (APL) muscles, two important stabilizers of the radial wrist in hominoid primates. Specifically, we used information available from previous dissections carried out by our team on 12 *H. sapiens* (seven males and five females), 8 *P. troglodytes* (three males and five females), 3 *G. gorilla* (two males and one female) and 3 *P. pygmaeus* (three females). The 12 human samples came from the Body Donation Service of the University of Barcelona and had an average age of 87.7 years (range, 81–94 years). All nonhuman primates were adults from the Anatomy Museum of the University of Valladolid. For each sample, we calculated the percentage of the weight of the FCR and APL muscles (%FCR and %APL) with respect to the total weight of the flexor and extensor muscles of the wrist (FCR, palmaris longus, flexor carpi ulnaris, flexor digitorum superficialis, flexor pollicis longus, flexor digitorum profundus, extensor carpi radialis longus, extensor carpi radialis brevis, extensor digitorum, extensor digiti minimi, extensor carpi ulnaris, APS, extensor pollicis brevis, extensor pollicis longus and extensor indicis). In *P. troglodytes*, *G. gorilla*, and *P. pygmaeus*, the flexor pollicis longus and extensor pollicis brevis muscles were not identified.

The non-parametric Mann–Whitney *U* test was used to compare RSC + LRLiss/DAS, SRLiss/DAS, RSC + LRLa, and SRLa among the four species of hominoid primates and to compare RSC + LRLw, SRLw, RSC + LRLw/R, SRLw/R, %RSC + LRL, %SRL, RSC + LRLs, SRLs, %FCR, and %APL between *H. sapiens* and *P. troglodytes*. No statistical comparisons were made of the %FCR and %APL values with *G. gorilla* or *P. pygmaeus* due to the small sample size of these two species. Statistical significance was set at $p < .05$. All analyses were performed with SPSS 22.

2.4 | Ethical note

This research complied with protocols approved by the Institutional Animal Care and Use Committee of the University of Barcelona and adhered to the legal requirements of Spain.

3 | RESULTS

3.1 | 3D GM analysis

The PCA yielded 23 principal components (PCs), three of which explained 62.8% of the variance in shape of the two ligament insertion sites: PC1, 34.9%; PC2, 16.1%; and PC3, 11.8%. The remaining components accounted for $\leq 6\%$ each. The scatter plot of PC1 versus PC2 (Figure 5) shows differences among the four species studied, although there is a clear degree of overlapping. *H. sapiens* showed more positive values for PC1, while the knuckle-walkers *P. troglodytes* and *G. gorilla*, showed more negative values and *P. pygmaeus* showed

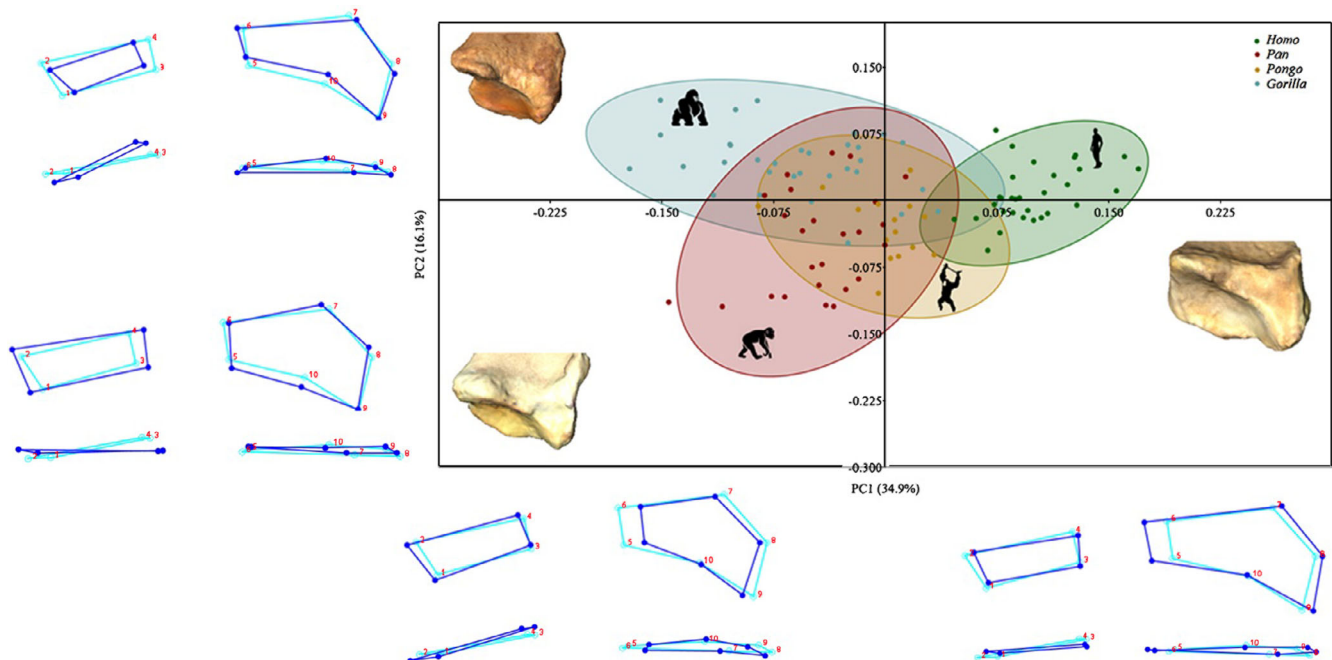


FIGURE 5 Scatter plot of PC1 versus PC2 derived from the PCA of the GM analysis. The ellipses include 95% confidence intervals of the group mean. Dark blue wireframes show the extreme shape of each PC in a palmar view (upper panel) and a proximal view (lower panel). Light blue wireframes represent the mean shape (coordinates 0.0). The 3D models of the distal radial epiphysis correspond to the individuals at the positive extreme of the PC1 (*Homo sapiens*), at the positive extreme of the PC2 (*Gorilla gorilla*), and the negative extreme of the PC2 (*Pan troglodytes*)

a PC1 intermediate values. PC2 was able to differentiate between the knuckle-walkers, with *G. gorilla* showing positive and *P. troglodytes* negative values for PC2. PC3 did not identify differences among the four species studied.

Shape changes on PC1 (Figure 5) indicate that the individuals with positive values have a relatively larger insertion site of the RSC + LRL ligaments, mainly due to the elongation of their ulnar region, and a relatively smaller and more palmarly oriented insertion site of the SRL ligament. In contrast, individuals with negative values have a relatively smaller insertion site of the RSC + LRL ligaments and a relatively larger and more ulnopalmarly oriented insertion site of the SRL ligament. Shape changes on PC2 (Figure 5) show that the size of the insertion site of the SRL ligament is relatively smaller and ulnopalmarly oriented in individuals with positive values. In individuals with negative PC2 values, the insertion site of the SRL ligament is relatively larger and more palmarly oriented.

The LDA revealed a significant difference for the Procrustes distance ($p < .001$) and the T-square test ($p < .001$) among all the species studied except between *P. troglodytes* and *P. pygmaeus*, where there were no significant differences for the T-square test ($p = .057$) (Tables 3 and 4). Leave-one-out cross validations showed that the *post hoc* probabilities of correct classification decreased in all the comparisons, except in the comparison between *H. sapiens* and *G. gorilla* (Table 5). The MRA of shape onto CS (Figure 6) was not significant for PC1 ($p = .34$) or for PC3 ($p = .94$), explaining these components the 46.7% of the total variance in shape of the two ligament insertion sites. Although the MRA of shape onto the CS was significant for PC2 ($p = .0004$), only 11.48% of the variance in shape of the two ligament insertion sites can be attributable to size. The MRA of shape onto DAS was significant for PC1 ($p < .001$), for PC2 ($p < .001$), and for PC3 ($p = .036$), but also in this case only a very low percentage of the variation of shape can be attributed to size differences (13.91% for PC1, 12.17% for PC2, and 6.95% for PC3).

TABLE 3 Mahalanobis and Procrustes (in italics) distances between groups with p values (in parenthesis) based on 1,000 permutations

Species	<i>Gorilla gorilla</i>	<i>Homo sapiens</i>	<i>Pan troglodytes</i>
<i>Homo sapiens</i>	8.54 (<0.0001)		
	0.17 (<0.0001)		
<i>Pan troglodytes</i>	4.91 (<0.0001)	7.07 (<0.0001)	
	0.10 (<0.0001)	0.16 (<0.0001)	
<i>Pongo pygmaeus</i>	6.47 (<0.0001)	7.94 (<0.0001)	3.56 (0.057)
	0.12 (<0.0001)	0.13 (<0.0001)	0.08 (<0.0001)

TABLE 4 T-square test between Procrustes distances

Species	<i>Gorilla gorilla</i>	<i>Homo sapiens</i>	<i>Pan troglodytes</i>
<i>Homo sapiens</i>	1,130.23 (<0.0001)		
<i>Pan troglodytes</i>	333.12 (<0.0001)	692.43 (<0.0001)	
<i>Pongo pygmaeus</i>	423.13 (<0.0001)	637.88 (<0.0001)	119.01 (0.057)

The 3D GM results were borne out by the quantitative values of the ligament insertion sites (Figure 7 and Table 6). RSC + LRL/DAS was higher in *H. sapiens* than in the other primates (Figure 7a); differences were significant for *P. troglodytes* (0.30 vs. 0.25; $p = .013$) but not for *G. gorilla* (0.30 vs. 0.26; $p = .098$) or *P. pygmaeus* (0.30 vs. 0.27; $p = .331$). SRL/DAS was lower in *H. sapiens* than in the other primates (Figure 7b); differences were significant for *P. pygmaeus* (0.16 vs. 0.30; $p < .001$) and *P. troglodytes* (0.16 vs. 0.41; $p < .001$) but not for *G. gorilla* (0.16 vs 0.21; $p = .082$). The ulnopalmarly oriented insertion site of the SRL ligament in individuals with PC1 negative values was reflected in the obtuse angle formed by the main axis of the insertion site with the transversal axis of the distal radial epiphysis in *P. troglodytes* and *G. gorilla* (165.9° and 157.9°), while in *H. sapiens* and *P. pygmaeus*, this insertion site has a radiopalmar orientation and an acute angle (7.2° and 9.5°) (Figures 4 and 7c). According to PC2 values, SRL/DAS was much lower in *G. gorilla* than in *P. troglodytes* (0.21 vs. 0.41; $p < .001$) (Figure 7b). *G. gorilla* also had a more ulnopalmarly oriented SRL insertion site, as indicated by the lower value of the SRLa parameter with respect to *P. troglodytes* (157.9° vs. 165.9°; $p < .001$) (Figures 4 and 7c). The orientation of the RSC + LRL insertion site was similar in all four species, as shown by 3D GM (Figure 5) and by RSC + LRLa values, indicating that all the species have a radiopalmar orientation, though with significant differences.

The phylogenetic correction showed that phylogeny is not associated with the shape of the ligament insertion sites based on the permutation test of the Procrustes aligned coordinates (phylogenetic signal, tree

TABLE 5 Percentages of *post-hoc* correct classification from the discriminant functions and after leave-one out cross-validation

	Discriminant functions	After cross-validation	Decrease in correct classification %
<i>Gorilla gorilla</i> – <i>Homo sapiens</i>	100	100	0
<i>Gorilla gorilla</i> – <i>Pan troglodytes</i>	96.7	89.2	–7.5
<i>Gorilla gorilla</i> – <i>Pongo pygmaeus</i>	100	86.9	–13.1
<i>Homo sapiens</i> – <i>Pan troglodytes</i>	100	96.4	–3.6
<i>Homo sapiens</i> – <i>Pongo pygmaeus</i>	100	95.6	–4.4
<i>Pongo pygmaeus</i> – <i>Pan troglodytes</i>	95	65	–30

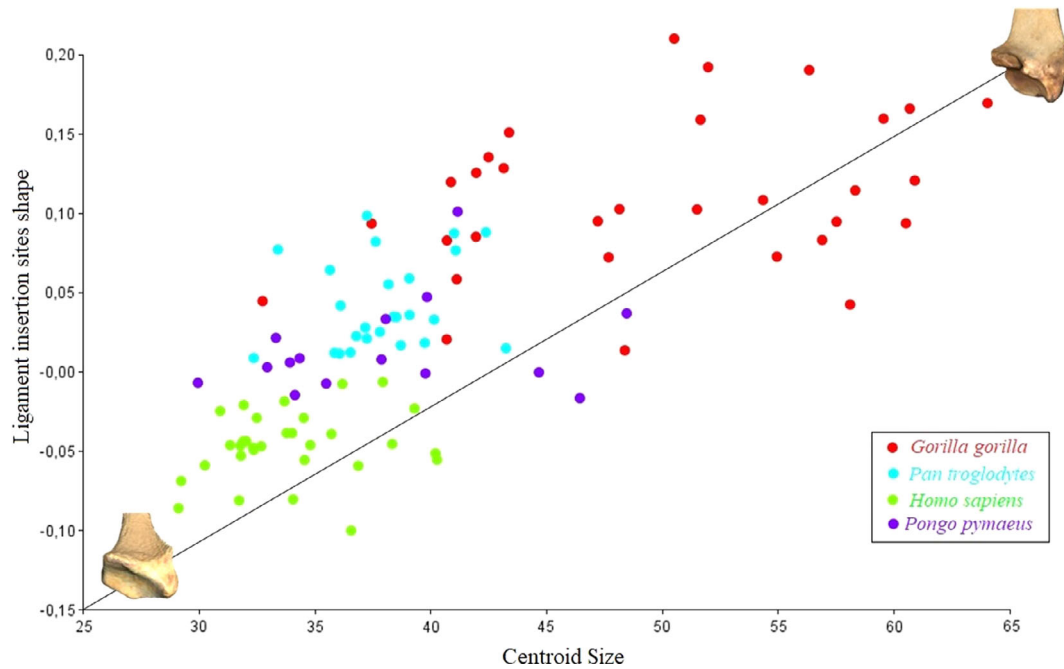


FIGURE 6 Scatter plot for the regression of shape onto the centroid size. The 3D models of the distal radial epiphysis correspond to individuals at the two extreme points of the regression

length = 0.02165067; $N = 102$; $p = .9613$) and the PC scores (phylogenetic signal, tree length = 0.02165067; $N = 102$; $p = .9606$).

3.2 | Ligament and muscle dissection

The results of the analyses of ligaments and muscles are summarized in Tables 7 and 8. The absolute weight of the RSC + LRL ligaments was greater in *H. sapiens* than in *P. troglodytes* (RSC + LRLw = 0.97 g vs. 0.88 g), while the absolute weight of the SRL ligament was greater in *P. troglodytes* than in *H. sapiens* (SRLw = 0.6 g vs. 0.4 g). However, these two differences are not statistically significant ($p = .329$ and $p = .177$, respectively). The percentage of absolute weight of the RSC + LRL ligaments with respect to the total weight of the radiocarpal joint ligaments was significantly higher in *H. sapiens* than in *P. troglodytes* (%RSC + LRL = 33.2% vs. 22.1%; $p = .004$), while the percentage of absolute weight of the SRL ligament was slightly but not significantly higher in *P. troglodytes* than in *H. sapiens* (%SRL = 14.7% vs. 13.4%; $p = .662$). When the absolute weights of the ligaments were normalized according to the size of the distal radius, the RSC + LRL ligaments were relatively but not significantly heavier in *H. sapiens* than in *P. troglodytes* (RSC + LRLw/R = 0.00133 vs. 0.00094; $p = .052$) and the SRL ligament was relatively but not significantly heavier in *P. troglodytes* than in *H. sapiens* (SRLw/R = 0.00063 vs. 0.00055; $p = .662$). The surface area of the RSC + LRL ligaments was larger in *H. sapiens* than in *P. troglodytes* (RSC + LRLs = 357.2 mm² vs. 332.5 mm²; $p = .792$) and the surface area of the SRL ligament was significantly higher in *P. troglodytes* than in *H. sapiens* (SRLs = 244.7 mm² vs. 113.9 mm²; $p = .009$).

The proportional weight of the FCR and APL muscles with respect to the total weight of the flexor and extensor muscles of the wrist was

significantly lower in *H. sapiens* than in *P. troglodytes* (%FCR = 5.6 vs. 9.0%; $p < .001$; %APL = 3.8% vs. 5.4%; $p = 0.012$). Proportional weights in *G. gorilla* were slightly higher (%FCR = 9.4%; %APL = 6.9%) than in *P. troglodytes*, while those for *P. pygmaeus* (%FCR = 7.5%; %APL = 4.4%) were midway between *H. sapiens* and the knuckle-walkers.

4 | DISCUSSION

The 3D GM analysis of the two ligament insertion sites in the distopalmar region of the distal radial epiphysis identified morphological differences among the different species of hominoid primates studied, which may be related to the types of locomotion developed by these species.

The most striking feature in *H. sapiens* was the relatively large insertion site of the RSC + LRL ligaments (Figure 5). These ligaments play an important role in stabilizing the radiocarpal joint in modern humans (Apergis, 2013; Cardoso & Szabo, 2007), since they limit the extension and ulnar deviation of the scaphoid and lunate during the extension and ulnar deviation of the wrist (Bateni et al., 2013; Nordin & Frankel, 2001; Ringler & Murthy, 2015; Short et al., 2002; Short et al., 2007). This functional importance of the two ligaments in humans reflects their histology, since they are composed of densely packed collagen fibers with little innervation, making them especially adapted to resist the axial loads transmitted through the radial region of the wrist (Hagert, 2010). At the same time, the functional importance of the RSC and LRL ligaments in humans also reflects the fact that they are more highly developed than the other ligaments of the wrist (Nordin & Frankel, 2001). This development of the RSC and LRL ligaments in *H. sapiens* can explain the relatively larger size of their

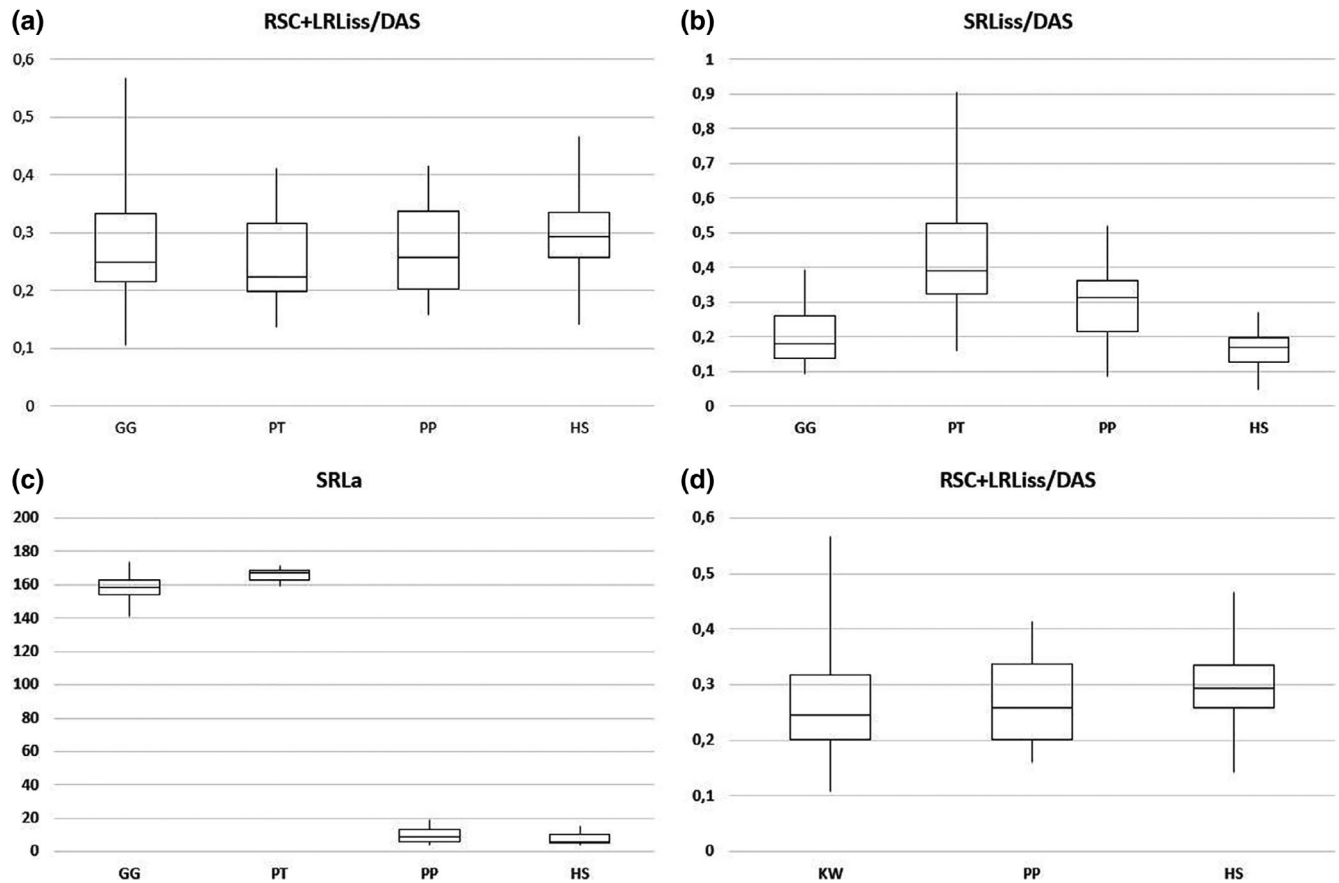


FIGURE 7 Box and whisker plots of the relative values of the surface areas of the ligament insertion sites in relation to the distal articular surface (a, b, and d) and the orientation angle of the SRL ligament insertion site (c). a, angle; DAS, distal articular surface; iss, insertion site surface; GG, *Gorilla gorilla*; HS, *Homo sapiens*; KW, knuckle-walker primates; PP, *Pongo pygmaeus*; PT, *Pan troglodytes*

TABLE 6 Mean and standard deviations (in parenthesis) of the quantitative analysis of the surface area and orientation of the insertion sites of the RSC + LRL and SRL ligaments in the four species of hominoid primates studied

	RSC + LRLiss/DAS	SRLiss/DAS	RSC + LRLa	SRLa
HS versus PP	0.30 (0.08) vs 0.27 (0.08)	0.16 (0.05) vs 0.30 (0.12)	22.0 (4.1) vs 19.0 (5.3)	7.2 (3.1) vs 9.5 (4.7)
	$p = .331$	$p < .001^*$	$p = .122$	$p = .066$
HS versus PT	0.30 (0.08) versus 0.25 (0.08)	0.16 (0.05) versus 0.41 (0.17)	22.0 (4.1) versus 20.7 (5.4)	7.2 (3.1) versus 165.9 (3.5)
	$p = .013^*$	$p < .001^*$	$p < .001^*$	$p = .453$
HS versus GG	0.30 (0.08) versus 0.26 (0.10)	0.16 (0.05) versus 0.21 (0.08)	22.0 (4.1) versus 30.0 (6.0)	7.2 (3.1) versus 157.9 (8.1)
	$p = .098$	$p = .082$	$p < .001^*$	$p < .001^*$
PP versus PT	0.27 (0.08) versus 0.25 (0.08)	0.30 (0.12) versus 0.41 (0.17)	19.0 (5.3) versus 20.7 (5.4)	9.5 (4.7) versus 165.9 (3.5)
	$p = .321$	$p = .018^*$	$p < .001^*$	$p = .305$
PP versus GG	0.27 (0.08) versus 0.26 (0.10)	0.30 (0.12) versus 0.21 (0.08)	19.0 (5.3) versus 30.0 (6.0)	9.5 (4.7) versus 157.9 (8.1)
	$p = .897$	$p = .010^*$	$p < .001^*$	$p < .001^*$
PT versus GG	0.25 (0.08) versus 0.26 (0.10)	0.41 (0.17) versus 0.21 (0.08)	20.7 (5.4) versus 30.0 (6.0)	165.9 (3.5) versus 157.9 (8.1)
	$p = .352$	$p < .001^*$	$p < .001^*$	$p < .001^*$

Abbreviations: a, angle; DAS, distal articular surface; GG, *Gorilla gorilla*; iss, insertion site surface; HS, *Homo sapiens*; PP, *Pongo pygmaeus*; PT, *Pan troglodytes*.

Asterisks indicate statistical significance.

insertion site, due mainly to its ulnar elongation, as seen in the 3D GM analysis (Figure 5) and in their higher RSC + LRLiss/DAS (Figure 7a and Table 6). This greater development of the RSC and LRL

ligaments in humans, which possibly affects the LRL ligament to a greater extent due to the morphological characteristics of its insertion site, as observed in our 3D GM analysis, is also reflected in the higher

TABLE 7 Results of the quantitative analysis of the palmar ligaments of the radiocarpal joint in *Homo sapiens* (HS) and *Pan troglodytes* (PT)

Sample	Age (years)	Sex	RSC + LRLw	SRLw	%RSC + LRL	%SRL	RSC + LRL/R	SRL/R	RSC + LRLs	SRLs
HS29B	83	M	0.99	0.49	26.8	13.2	0.00127	0.00063	361.4	187.2
HS73B	88	M	0.81	0.33	33.2	13.5	0.00105	0.00043	323.0	101.3
HS91B	81	M	0.99	0.20	35.4	7.1	0.00127	0.00026	353.6	76.4
HS40BF	81	M	0.90	0.59	28.1	18.4	0.00119	0.00078	361.6	142.1
HS132RS	94	F	1.09	0.26	36.8	8.8	0.00157	0.00037	418.7	68.6
HS9RC	92	F	1.04	0.52	38.8	19.4	0.00163	0.00082	324.9	107.7
Mean			0.97	0.40	33.2	13.4	0.00133	0.00055	357.2	113.9
SD			0.10	0.16	4.8	4.9	0.00022	0.00023	34.8	44.3
PT05	A	F	1.18	0.68	24.7	14.2	0.00140	0.00081	386.7	217.6
PT06	A	F	0.81	0.69	19.7	16.7	0.00089	0.00075	333.5	258.2
PT07	A	M	0.85	0.43	24.1	12.1	0.00085	0.00043	276.7	238.4
PT08	A	F	0.59	0.30	20.9	10.5	0.00062	0.00031	237.3	148.8
PT09	A	F	0.96	0.90	21.2	19.9	0.00091	0.00085	428.3	360.4
Mean			0.88	0.60	22.1	14.7	0.00094	0.00063	332.5	244.7
SD			0.22	0.24	2.2	3.7	0.00029	0.00024	77.9	76.7
			$p = .329$	$p = .177$	$p = .004^*$	$p = .662$	$p = .052$	$p = .662$	$p = .792$	$p = .009^*$

Abbreviations: F, female; M, male; SD, standard deviation.

Asterisks indicate statistical significance. Other abbreviations are defined in the text.

values for RSC + LRLw, %RSC + LRL, RSC + LRL/R, and RSC + LRLs in *H. sapiens* compared to *P. troglodytes* that we have observed in our samples.

The morphological analysis of the distal radial epiphysis indicated that *P. pygmaeus* has a smaller insertion site of the RSC + LRL ligaments than *H. sapiens*, as shown by the PC1 of the 3D GM (Figure 5) and by the lower RSC + LRL/DAS (Figure 7a and Table 6). This lesser development of the RSC + LRL ligaments is compensated by the larger SRL insertion site, as shown by 3D GM (Figure 5) and by the higher SRL/DAS in *P. pygmaeus* (Figure 7b and Table 6). The greater development of the SRL ligament in *P. pygmaeus* may be related to its arboreal locomotion, especially vertical climbing, which requires a marked ulnar deviation of the hand (Sarmiento, 1988). This ulnar deviation of the wrist during vertical climbing puts heavy loads on the wrist, particularly on the radiolunate joint (Heinrich et al., 1993; Richmond et al., 2001). This extra load is compensated for by a greater development of its main stabilizing element, the SRL ligament.

The knuckle-walkers had a relatively smaller RSC + LRL insertion site than *H. sapiens*, as shown by the negative PC1 values (Figure 5) and by the lower RSC + LRL/DAS in *P. troglodytes* and *G. gorilla* than in *H. sapiens* (Figure 7a and Table 6). This lesser development of the RSC + LRL ligaments in the knuckle-walkers is reflected in the lower RSC + LRLw, %RSC + LRL, RSC + LRL/R, and RSC + LRLs values observed in *P. troglodytes*. This could be related to the greater stability of the scaphoid and semilunar bones in these primates, which translates in a reduced mobility during wrist extension (Orr, 2017) and a lesser need for a large ligament to ensure stability.

The morphological analysis of the SRL ligament insertion site differentiated between the two species of knuckle-walkers. The morphology

of *P. troglodytes* was closer to *P. pygmaeus* than to *G. gorilla*. This similarity between *P. troglodytes* and *P. pygmaeus* despite their different locomotor behavior, may be due to the fact that *P. troglodytes* is the more arboreal African great ape of the two represented in this study and has developed different types of arboreal locomotion, including vertical climbing, quadrupedal walking in trees, and suspensory locomotion like brachiation (Hunt, 1991; Hunt, 1992). As indicated by the PC2 values (Figure 5), *P. troglodytes* has a larger SRL insertion site and a correspondingly higher SRL/DAS than *G. gorilla* (Figure 7b and Table 6). This development of the SRL ligament in chimpanzees is reflected in the higher SRLw, %SRL, SRLw/R, and SRLs values that we have observed in our *P. troglodytes* compared to our *H. sapiens* specimens. This could be related to vertical climbing, since it would compensate for the extra loads on the radiolunate joint (Heinrich et al., 1993; Richmond et al., 2001), as occurs in *P. pygmaeus*. The smaller SRL insertion site in *G. gorilla* compared to *P. troglodytes* may also be related to possible differences between the two species in their knuckle-walking styles. Kivell and Schmitt (2009) postulated that while *P. troglodytes* extend their wrist during the support phase of knuckle-walking, *G. gorilla* use a columnar posture of the upper extremity with a neutral position of the wrist, which entails less movement of the lunate and, thus, a lesser development of its stabilizing ligaments.

The ulnopalmar orientation of the SRL ligament insertion site in African great apes, as indicated by their position among the negative values of PC1 (Figure 5), could be encompassed within the combination of adaptations of the distal radius that stabilizes the radiocarpal joint of the knuckle-walker primates, thereby facilitating their weight-bearing, slightly extended wrist posture (Kivell, 2016). In our opinion, the reorientation of the SRL ligament could imply a premature tension of the

TABLE 8 Proportional weight of the flexor carpi radialis (FCR) and abductor pollicis longus (APL) muscles with respect to the other stabilizing muscles of the wrist in *Homo sapiens* (HS) and *Pan troglodytes* (PT)

Sample	Age (years)	Sex	%FCR	%APL
HS01B	85	M	4.6	3.8
HS29B	83	M	6.5	3.7
HS91B	81	M	4.6	3.7
HS4BF	91	M	6.4	3.0
HS40BF	81	M	5.7	4.7
HS38BF	85	M	5.3	3.3
HS60G	93	F	5.5	3.1
HS86BF	91	M	6.4	3.8
HS132RS	94	F	5.5	4.1
HS108G	85	F	6.3	4.1
HS9RC	92	F	5.7	3.5
HS7RC	91	F	4.7	4.9
Mean			5.6	3.8
SD			0.7	0.6
PT02	A	F	8.2	4.6
PT03	A	M	8.9	3.2
PT04	A	M	10.2	5.9
PT05	A	F	8.4	3.8
PT06	A	F	8.9	6.6
PT07	A	M	9.8	5.9
PT08	A	F	8.3	7.1
PT09	A	F	9.3	6.3
Mean			9.0	5.4
SD			0.7	1.4
			$p < .001^*$	$p = .012^*$

Abbreviations: F, female; M, male; SD, standard deviation. Asterisks indicate statistical significance. Other abbreviations are defined in the text.

ligament during wrist extension, which would help to prevent its collapse during knuckle-walking (Richmond & Strait, 2000). However, it is necessary to undertake a precise biomechanical analysis of the wrist ligaments in knuckle-walker primates in order to confirm this view. On the other hand, the greater ulnopalmar orientation of the SRL insertion site in *G. gorilla* compared to *P. troglodytes* (Figures 4 and 5) can be explained by the less frequent use of vertical climbing in gorillas, especially in the adult (Doran, 1993; Remis, 1995). The heavy load on the radiolunate joint during vertical climbing (Heinrich et al., 1993; Richmond et al., 2001) are compensated for in *P. troglodytes* and *P. pygmaeus* by an increase in the dorsopalmar and mediolateral diameters of the lunate in these species (Kivell et al., 2013). Thus, the larger size of the lunate in *P. pygmaeus* and *P. troglodytes* would clearly displace the ulnar edge of the insertion site of the SRL ligament, which would explain the more palmar orientation in these two species compared to *G. gorilla*. The greater palmar orientation of the SRL insertion site in *P. troglodytes* is reflected in a higher SRLa compared to *G. gorilla* (Figure 7c and Table 6).

The differences in size that we have observed in the insertion site of the RSC + LRL ligaments in our four species of primates may also be related to anatomic characteristics of the muscles that stabilize the wrist. The FCR and the APS play an important role in stabilizing the radial and palmar region of the wrist and assist the RSC + LRS ligaments in stabilizing the scaphoid (Esplugas, Garcia-Elias, Lluch, & Llusá, 2016; Whitehead, 1993). Our 3D GM analysis revealed a progression from largest to smallest relative size of the insertion site of the RSC + LRL ligaments among *H. sapiens* > *P. pygmaeus* > knuckle-walker primates. This progression was confirmed by RSC + LRL/DAS values (Figure 7d and Table 6), where *H. sapiens* had the highest values and *P. pygmaeus* had values slightly higher than the knuckle-walkers. This progression mirrors the inverse progression that we observed when analyzing the proportional weight of the FCR and APL muscles with respect to the total weight of the stabilizing muscles of the wrist (knuckle-walker primates > *P. pygmaeus* > *H. sapiens*). The lesser development of the FCR and APL muscles corresponds to a relatively larger size of the insertion site of the RSC + LRL ligaments and, thus, with a greater development of these ligaments, as we have seen when comparing the RSC + LRL ligaments of *H. sapiens* with *P. troglodytes*. This would explain the fact that humans have a relatively larger insertion site of the RSC + LRL ligaments compared to the other hominoid primates (Figure 7a).

In conclusion, our 3D GM analysis has identified morphological differences in the insertion sites of the RSC + LRL and SRL ligaments between *H. sapiens*, *P. pygmaeus*, *P. troglodytes* and *G. gorilla* that reflect their different types of locomotion. However, the differences observed have a greater effect on the relative size and orientation of the ligament insertion sites rather than their intrinsic form, as is demonstrated by the quantitative analysis. The differences observed in the two ligament insertion sites in the distal radius correlate with the absolute and relative size of the corresponding ligaments in *H. sapiens* and *P. troglodytes*, although some of the differences are not statistically significant, possibly due to our small sample size. Therefore, in order to confirm that the results obtained in our 3D GM analysis correspond to the anatomic characteristics of the palmar ligaments of the radiocarpal joint, it would be necessary to expand our data by including more specimens of *P. troglodytes* and *H. sapiens* and to acquire data on *P. pygmaeus* and *G. gorilla*. Nevertheless, our findings can expand our current knowledge on the functional anatomy of the bones, ligaments, and muscles in the wrists of hominoid primates and can provide innovative data that will help assign a particular type of locomotion to extinct primates based on fossilized fragments of the distal epiphysis of the radius.

ACKNOWLEDGMENTS

We would like to thank Manuel Martín, Sebastián Mateo, and Pau Rigol (Body Donation Service, University of Barcelona) and Joshua Martín for their support and collaboration. We thank Renee Grupp for assistance in drafting the manuscript. We would also like to thank Marcia Ponce de León and Christoph P. E. Zollikofer (University of Zurich Anthropological Institute and Museum) for their advice and kindness and for granting us access to the material under their care. This study was funded by the Ministerio de Economía y Competitividad of Spain (project CGL2014-52611-C2-2-P

to JMP), by the European Union (FEDER) and by the Ajudes Predoctorals of the University of Barcelona (APIF-UB 2016/2017 to AC).

CONFLICT OF INTEREST

The authors declare that they have no conflict of interest.

AUTHOR CONTRIBUTIONS

J.M.P., A.C., V.P., M.B., F.J.P., and J.F.P. dissected the human and the chimpanzee samples. A.C., M.G., and M.D. performed the 3D GM analysis. All the authors participated in the study design, in the collection, analysis, and interpretation of data, in the writing and review of the manuscript and in the decision to submit the article for publication.

ORCID

Josep M. Potau  <https://orcid.org/0000-0003-3387-8760>

REFERENCES

- Almécija, S., & Alba, D. (2014). On manual proportions and pad-to-pad precision grasping in *Australopithecus afarensis*. *Journal of Human Evolution*, 73, 88–92.
- Apergis, E. (2013). *Fracture-dislocations of the wrist*. Milan: Springer.
- Arias-Martorell, J., Potau, J. M., Bello-Hellegouarch, G., Pastor, J. F., & Pérez-Pérez, A. (2012). 3D geometric morphometric analysis of the proximal epiphysis of the hominoid humerus. *Journal of Anatomy*, 221, 394–405.
- Arnold, C., Matthews, L. J., & Nunn, C. L. (2010). The 10kTrees website: A new online resource for primate phylogeny. *Evolutionary Anthropology*, 19, 114–118.
- Batani, C. P., Bartolotta, R. J., Richardson, M. L., Mulcahy, H., & Allan, C. H. (2013). Imaging key wrist ligaments: What the surgeon needs the radiologist to know. *American Journal of Roentgenology*, 200, 1089–1095.
- Berger, R. A. (2010). In W. Cooney (Ed.), *Wrist anatomy*. Philadelphia: Lippincott Williams & Wilkins.
- Bookstein, F. L. (1991). *Morphometric tools for landmark data: Geometry and biology*. Cambridge: Cambridge University Press.
- Buijze, G. A., Dvinskikh, N. A., Strackee, S. D., Streekstra, G. J., & Blankevoort, L. (2011). Osseous and ligamentous scaphoid anatomy: Part II. Evaluation of ligament morphology using threedimensional anatomical imaging. *Journal of Hand Surgery*, 36, 1936–1943.
- Buijze, G. A., Lozano-Calderon, S. A., Strackee, S. D., Blankevoort, L., & Jupiter, J. B. (2011). Osseous and ligamentous scaphoid anatomy: Part I. A systematic literature review highlighting controversies. *Journal of Hand Surgery*, 36, 1926–1935.
- Cardoso, R., & Szabo, R. M. (2007). Wrist anatomy and surgical approaches. *Orthopedic Clinics of North America*, 38, 127–148.
- Cignoni, P., Callieri, M., Corsini, M., Dellepiane, M., Ganovelli, F., & Ranzuglia, G. (2008). MeshLab: an open-source mesh processing tool. In V. Scarano, R. De Chiara, & U. Erra (Eds.), *6th Eurographics Italian Chapter Conference* (pp. 129–136).
- Doran, D. M. (1993). Comparative locomotor behavior of chimpanzees and bonobos: The influence of morphology on locomotion. *American Journal of Physical Anthropology*, 91, 83–98.
- Espuglas, M., Garcia-Elias, M., Lluç, A., & Llusà, M. (2016). Role of muscles in the stabilization of ligament-deficient wrists. *Journal of Hand Therapy*, 29(2), 166–174.
- Gebo, D. L. (2014). *Primate comparative anatomy*. Baltimore: Johns Hopkins University Press.
- Hagert, E. (2010). Proprioception of the wrist joint: A review of current concepts and possible implications on the rehabilitation of the wrist. *Journal of Hand Therapy*, 23, 2–17.
- Heinrich, R. E., Rose, M. D., Leakey, R. E., & Walker, A. C. (1993). Hominid radius from the Middle Pliocene of Lake Turkana, Kenya. *American Journal of Physical Anthropology*, 92, 139–148.
- Hunt, K. D. (1991). Mechanical implications of chimpanzee positional behavior. *American Journal of Physical Anthropology*, 86, 521–536.
- Hunt, K. D. (1992). Positional behavior of *Pan troglodytes* in the Mahale mountains and Gombe Stream National Parks, Tanzania. *American Journal of Physical Anthropology*, 87, 83–105.
- Jenkins, F. A. J., & Fleagle, J. G. (1975). In R. Tuttle (Ed.), *Knuckle-walking and the functional anatomy of the wrists in living apes*. The Hague: Mouton.
- Katz, D. A., Green, J. K., Werner, F. W., & Loftus, J. B. (2003). Capsuloligamentous restraints to dorsal and palmar carpal translation. *Journal of Hand Surgery*, 28, 610–613.
- Kivell, T. L. (2016). In T. L. Kivell, P. Lemelin, B. G. Richmond, & D. Schmitt (Eds.), *The primate wrist*. New York: Springer.
- Kivell, T. L., Barros, A. P., & Smaers, J. B. (2013). Different evolutionary pathways underlie the morphology of wrist bones in hominoids. *BMC Evolutionary Biology*, 13, 229.
- Kivell, T. L., & Schmitt, D. (2009). Independent evolution of knuckle-walking in African apes shows that humans did not evolve from a knuckle-walking ancestor. *Proceedings of the National Academy of Sciences*, 106, 14241–14246.
- Klingenberg, C. P. (2011). MorphoJ: An integrated software package for geometric morphometrics. *Molecular Ecology Resources*, 11, 353–357.
- Mayfield, J. K., Williams, W. J., Erdman, A. G., Dahlof, W. J., Wallrich, M. A., Kleinhenz, W. A., & Moody, N. R. (1979). Biomechanical properties of human carpal ligaments. *Orthopaedic Transactions*, 3, 143–144.
- Nordin, M., & Frankel, V. H. (2001). *Basic biomechanics of the musculoskeletal system*. Baltimore: Lippincott Williams and Wilkins.
- O'Higgins, P. (2000). The study of morphological variation in the hominid fossil record: Biology, landmarks and geometry. *Journal of Anatomy*, 197, 103–120.
- Orr, C. M. (2017). Locomotor hand postures, carpal kinematics during wrist extension, and associated morphology in anthropoid primates. *Anatomical Record*, 300, 382–401.
- Perelman, P., Johnson, W. E., Roos, C., Seuánez, H. N., Horvath, J. E., Moreira, M. A. M., ... Pecon-Slattey, J. (2011). A molecular phylogeny of living primates. *PLoS Genetics*, 7, e1001342.
- Remis, M. (1995). Effects of body size and social context on the arboreal activities of lowland gorillas in the Central African Republic. *American Journal of Physical Anthropology*, 97, 413–433.
- Richmond, B. G., Begun, D. R., & Strait, D. S. (2001). Origin of human bipedalism: The knuckle-walking hypothesis revisited. *Yearbook of Physical Anthropology*, 44, 70–105.
- Richmond, B. G., & Strait, D. S. (2000). Evidence that humans evolved from a knuckle-walking ancestor. *Nature*, 404, 382–385.
- Ringler, M. D., & Murthy, N. S. (2015). MR imaging of wrist ligaments. *Medical Clinics of North America*, 23, 367–391.
- Rohlf, F. J., & Marcus, L. (1993). A revolution in morphometrics. *Trends in Ecology & Evolution*, 8, 129–132.
- Rueden, C. T., Schindelin, J., Hiner, M. C., DeZonia, B. E., Walter, A. E., Arena, E. T., & Eliceiri, K. W. (2017). ImageJ2: ImageJ for the next generation of scientific image data. *BMC Bioinformatics*, 18, 529.
- Sarmiento, E. E. (1988). Anatomy of the hominoid wrist joint: Its evolutionary and functional implications. *International Journal of Primatology*, 9, 281–345.
- Short, W. H., Werner, F. W., Green, J. K., & Masaoka, S. (2002). Biomechanical evaluation of ligamentous stabilizers of the scaphoid and lunate. *Journal of Hand Surgery*, 27, 991–1002.

- Short, W. H., Werner, F. W., Green, J. K., Sutton, L. G., & Brutus, J. P. (2007). Biomechanical evaluation of the ligamentous stabilizers of the scaphoid and lunate: Part III. *Journal of Hand Surgery*, 32, 297–309.
- Tallman, M. (2012). Morphology of the distal radius in extant hominoids and fossil hominins: Implications for the evolution of bipedalism. *Anatomical Record*, 295, 454–464.
- Thorpe, S. K. S., & Crompton, R. H. (2007). Origin of human bipedalism as an adaptation for locomotion on flexible branches. *Science*, 316, 1328–1331.
- Tuttle, R. H. (1967). Knuckle-walking and the evolution of hominoid hands. *American Journal of Physical Anthropology*, 26, 171–206.
- Tuttle, R. H. (1969). Knuckle-walking and the problem of human origins. *Science*, 166, 953–961.
- Whitehead, P. F. (1993). In D. L. Gebo (Ed.), *Aspects of the anthropoid wrist and hand*. Illinois: Northern Illinois University Press.
- Wiley, D. F. (2006). *Landmark editor 3.0*. Davis: IDAV, University of California. <http://graphics.idav.ucdavis.edu/research/EvoMorph>
- Zelditch, M. L., Swiderski, D. L., Sheets, H. D., & Fink, W. L. (2004). *Geometric morphometrics for biologists: A primer*. New York: Academic Press.

How to cite this article: Casado A, Punsola V, Gómez M, et al. Three-dimensional geometric morphometric analysis of the distal radius insertion sites of the palmar radiocarpal ligaments in hominoid primates. *Am J Phys Anthropol*. 2019; 170:24–36. <https://doi.org/10.1002/ajpa.23885>